

Bouncing Outer Billiards

Andrey Gogolev

Levi Keck

Kevin Lewis

Received 09 Mar 2025; Accepted 22 Jul 2025

Abstract: We introduce a new class of billiard-like system, “bouncing outer billiards”, which are 3-dimensional cousins of outer billiards of Neumann and Moser. We prove that the bouncing outer billiards system on a smooth convex body has at least four 1-parameter families of fixed points. We also fully describe the dynamics of bouncing outer billiards on a line segment. Finally, we carry out numerical experiments suggesting very complicated (non-ergodic) behavior for several shapes, including the square and an ellipse.

AMS Classification: 37A10, 37C05, 37C25

Key words and phrases: Billiards, outer billiards, integrable systems, periodic orbits, numerical experiments

1 Introduction

Outer billiards are dynamical systems introduced by Neumann in 1959 [Neu58] and then popularized by Moser in his lecture on stability of the solar system [Mos73, Mos78].

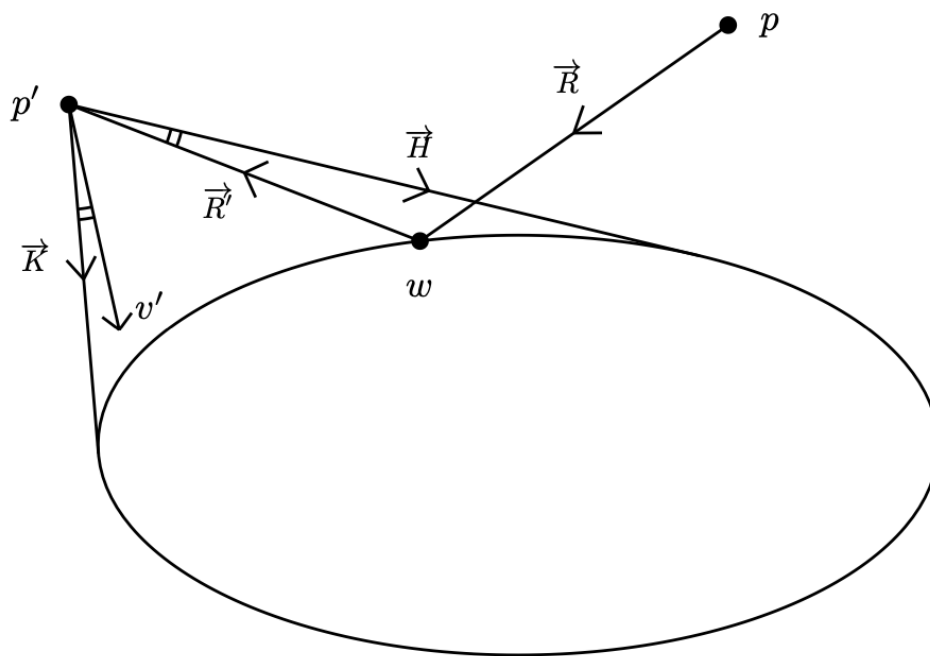


Figure 1: Bouncing Outer Billiards Dynamics

The field of outer billiards became very active about 20 years ago. In this paper, we suggest similar more complicated billiard systems called *bouncing outer billiards*, which we proceed to define.

Let $S \subset \mathbb{R}^2$ be a compact convex set with smooth boundary. The *visibility domain* V_S consists of all pairs (p, v) where $p \in \mathbb{R}^2 \setminus \text{int}(S)$, and $v \in T_p^1 \mathbb{R}^2$ is a unit vector based at p such that the ray \vec{R} spanned by v has a nonempty intersection with S .

We now define the dynamical system $F_S : V_S \rightarrow V_S$ in the following way. Given an initial condition $(p, v) \in V_S$ the corresponding ray \vec{R} reflects off the convex body at a point w as \vec{R}' in the usual way — the angle of incidence equals the angle of reflection. Next we apply the outer billiard law and consider the point $p' \in \vec{R}'$ such that $\|p - w\| = \|p' - w\|$ as indicated in Figure 1.

Finally, we will use the *visibility angle reflection rule* as follows. Let \vec{H} and \vec{K} be the rays at p' which are tangent to S . Let u be the unit vector based at p' pointing to w (in the

direction opposite to \vec{R}'). Clearly, u is inside the angle defined by \vec{H} and \vec{K} . Let v' be the reflection of u across the angle bisector of $\angle(\vec{H}, \vec{K})$ as shown on Figure 1. This completes the definition of bouncing billiard dynamics.

$$F_S(p, v) = (p', v').$$

We will drop the subscript S and simply write F when no confusion is possible.

Remark 1.1. *It is easy to see that if \vec{R} is tangent to S then we have the classical outer billiard dynamics. Hence, the outer billiard is simply the restriction $F|_{\partial V_S}$ of the bouncing outer billiard to the boundary of the visibility space.*

Remark 1.2 If S is not smooth, e.g. a polygon, then the angle reflection law is undefined for some initial conditions. However, such initial conditions form a set of zero Lebesgue measure since the boundary of a convex body is differentiable almost everywhere. Hence, bouncing billiard dynamics still makes sense for almost every initial condition, but the above relation to outer billiard is obscured.

Remark 1.3 S. Tabachnikov considered unfolding the outer billiard map into a family of symplectomorphisms given by the first two steps in the definition of the bouncing outer billiard [Tab95]. However, to the best of our knowledge, the visibility angle reflection rule was not considered before.

In the next section, we establish the existence of families of fixed points for bouncing outer billiards. Then, we fully describe integrable twist map dynamics of bouncing outer billiards on a line segment. Finally, we present results of our numerical explorations in the last section.

We would like to pose two questions.

Question 1.2. *Does every orbit of the bouncing outer billiard on a smooth convex body remain bounded?*

We were not able to detect any unbounded orbits numerically.

It is easy to check that bouncing outer billiards are conservative, that is, they preserve the Lebesgue measure on V_S (see Appendix A).

Question 1.3. *Does there exist positive volume ergodic components?*

We have found some orbits which appear to fill up 2-dimensional sets. However, in the 3-dimensional space V_S , such orbits seem to be confined to 2-dimensional surfaces.

Acknowledgements. This paper is a result of an REU project of summer 2024 at The Ohio State University. The authors are very grateful to Sergei Tabachnikov who provided several illuminating remarks on earlier drafts. The authors would like to acknowledge the support provided by the NSF grant DMS-2247747.

2 Fixed points

A natural question for any dynamical system is whether or not there exist fixed points, and if so, how to find them.

Theorem 2.1. *For any convex S with C^3 boundary, the associated billiard map has uncountably many fixed points, which come in at least four local 1-parameter families.*

Clearly, a point (p, v) can only be a fixed point if v is the bisector of the angle formed by the tangent rays from p to S . Therefore, given a point $p \notin S$, consider the angle given by the two tangent lines from p to S and let $v_p \in T_p \mathbb{R}^2$ be the vector spanning the angle bisector. The idea of the proof is to find a curve connecting two points, say p and q such that the ray of v_p “bounces to the left” and the ray of v_q “bounces to the right.” Then, by the intermediate value theorem, there exists a fixed point (r, v_r) on such a curve.

We note right away that if ∂S has a circle subarc with constant curvature, then there is a whole 2-parameter family of fixed points in proximity of such arc. Hence we can assume, due to C^3 regularity of the boundary, that there exists a subarc of ∂S with strictly increasing curvature, as well as a subarc with strictly decreasing curvature.

The following is our main lemma.

Lemma 2.2. *Let $f : [s_0, s_2] \rightarrow \partial S$ be a counter-clockwise arc-length parameterization of a subarc of ∂S along which the curvature is strictly increasing. Assume that this arc is sufficiently short so that the tangent lines at $f(s_0)$ and $f(s_2)$ intersect at a point p as indicated on Figure 2.*

Then the angle bisector ray spanned by v_p will “bounce off in the direction of $f(s_0)$ ”, that is, after reflecting off S , the ray will intersect the tangent segment a .

Proof. Let $k(s)$ be the curvature at $f(s)$, and let $K(s) = \int_{s_0}^s k(t)dt$. Since we are using arc-length parameterization, $K(s)$ is the angle between the tangent lines at $f(s_0)$ and $f(s)$. There is a unique s_1 such that $K(s_1) = K(s_2)/2$. Then the tangent line at $f(s_1)$ is perpendicular to v_p . Hence, to prove the claim of the lemma it suffices to show that the distance from $f(s_1)$ to the tangent line b is less than the distance from $f(s_1)$ to the tangent line a . This can be expressed by the following inequality:

$$\int_{s_1}^{s_2} \sin(K(s_2) - K(s))ds < \int_{s_0}^{s_1} \sin(K(s))ds \quad (*)$$

To prove this inequality, we can start with the following statements by change of variables:

$$\begin{aligned} \int_{s_1}^{s_2} \sin(K(s_2) - K(s))k(s)ds &= \int_0^{K(s_1)} \sin(u)du \\ \int_{s_0}^{s_1} \sin(K(s))k(s)ds &= \int_0^{K(s_1)} \sin(v)dv \end{aligned}$$

This gives

$$\int_{s_1}^{s_2} k(s) \sin(K(s_2) - K(s))ds = \int_{s_0}^{s_1} k(s) \sin(K(s))ds$$

Since curvature $k : [s_0, s_2] \rightarrow \mathbb{R}_+$ is increasing the posited inequality follows proving the lemma. \square

Proof of Theorem 2.1. Consider a local minimum (or maximum) of the curvature of ∂S . (By the 4-vertex theorem at least four local extrema exist.) On one side there is a short arc with increasing curvature and on the other side there is short arc with decreasing curvature. Applying the above lemma to the first arc we obtain an initial condition (p, v_p)

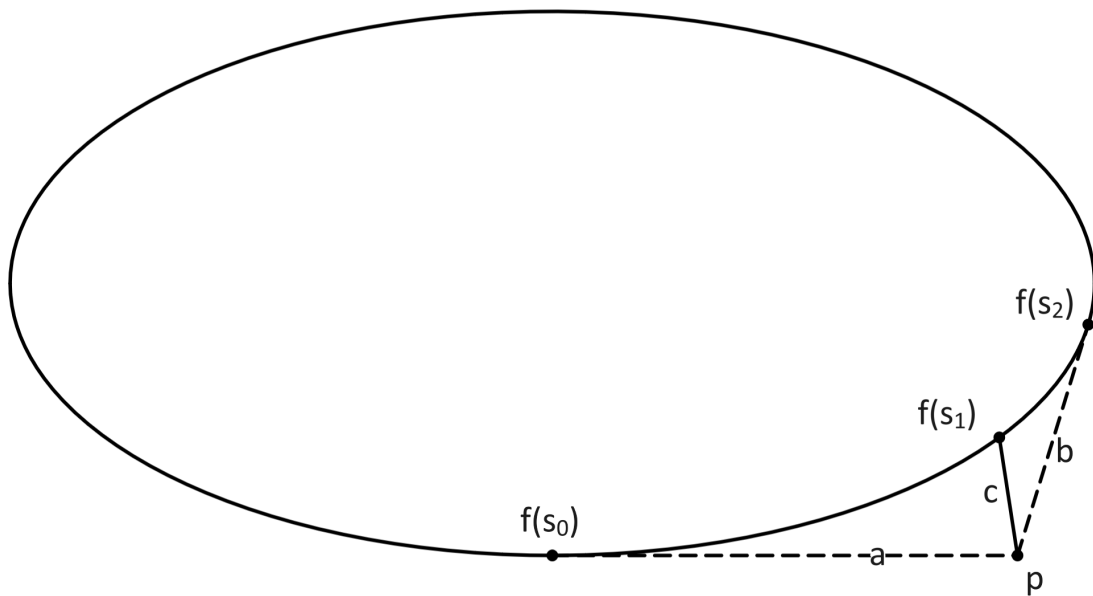


Figure 2: Fixed Point Lemma Setup

which “bounces to the left” and similarly, applying (the analogue of) the lemma to the arc with increasing curvature we obtain an initial condition (q, v_q) which “bounces to the right.” It remains to connect p and q by an arc disjoint with S and apply the intermediate value theorem. \square

It is clear from the above proof that each vertex of ∂S yields a 1-parameter family of fixed points. These families could merge away from S . We would like to pose the following question.

Question 2.3. *Let S be a convex domain with C^3 boundary. Does every closed curve around it contain at least one fixed point of the bouncing outer billiard map on S ?*

S. Tabachnikov considered a question of very similar flavor and eventually found a counterexample [Tab12].

3 Bouncing on a Line Segment

3.1 Parameterizing the Dynamics

This section focuses on the behavior of the bouncing outer billiards system on a line segment. Since all segments are congruent up to scaling, we only consider the segment on the x -axis from -1 to 1. For convenience, we will consider only initial points p with positive y -values, as points with negative y -values are symmetric.

Recall that we denote the visibility domain by V . Consider initial condition $(p, v) \in V$, where $p = (x, y)$, and let $\theta = \arg(v) + \frac{\pi}{2}$. The initial conditions define a ray from the point p with slope $\tan(\theta - \frac{\pi}{2})$. Using this equation, we can derive:

$$w = (x + y \tan(\theta), 0)$$

$$p' = (x', y') = (x + 2y \tan(\theta), y)$$

Note that the y -coordinate of the initial point will remain constant on the orbit. From this point forward, we will refer to the y -value of the initial point as height and denote it by h .

Next, we obtain that the angle from p' to the left and right endpoints of the segment are given by $\arctan\left(\frac{1-x'}{h}\right)$ and $\arctan\left(\frac{-1-x'}{h}\right)$, respectively. Also, the angle from p' to w is given by $-\theta$. Applying the visibility angle reflection rule yields:

$$\theta' = \arctan\left(\frac{1-x'}{h}\right) + \theta + \arctan\left(\frac{-1-x'}{h}\right)$$

Summing up, the dynamics, $F(x, h, \theta) = (x', h, \theta')$ is given by:

$$\begin{aligned} x' &= x + 2h \tan(\theta) \\ \theta' &= \theta + \arctan\left(\frac{1-x'}{h}\right) + \arctan\left(\frac{-1-x'}{h}\right) \end{aligned} \tag{1}$$

3.2 A Second Invariant

In Section 3.1, we observed that the height h is invariant. In this section, we will demonstrate the existence of a second invariant.

We define a new coordinate system in which it becomes easier to see a second invariant. First, consider the change of coordinates $g(x, h, \theta) = (w, h, d)$ given by

$$\begin{cases} w = x + h \tan(\theta) \\ d = h \tan(\theta) \end{cases} \tag{2}$$

with the h -coordinate remaining unchanged. The coordinate w represents the x -value of the bounce point and the coordinate d represents the signed difference between the w and the x -value of the initial point. The inverse coordinate transformation is given by:

$$\begin{cases} x = w - d \\ \theta = \arctan\left(\frac{d}{h}\right) \end{cases} \tag{3}$$

Now, we seek to understand the dynamics in these new coordinates. Let $f(w, h, d) = g \circ F \circ g^{-1}(w, h, d)$. We let $f(w, h, d)$ be denoted by (w', h, d') , which we wish to write in terms of w, h , and d . First, combining (1) and (2) yields:

$$x' = w + d \quad (4)$$

Now, we will use (1) to rewrite the equation for d' . Following this, we simplify and use (2) and (4) to rewrite all instances of x' and $h \tan(\theta)$ in terms of w and d .

$$\begin{aligned} d' &= h \tan(\theta') \\ &= h \tan\left(\theta + \arctan\left(\frac{1-x'}{h}\right) + \arctan\left(\frac{-1-x'}{h}\right)\right) \\ &= h \left(\frac{\tan(\theta) + \frac{-2x'h}{1+h^2-(x')^2}}{1 + \frac{2x'h}{1+h^2-(x')^2}} \right) \\ &= \frac{h \tan(\theta) + h^3 \tan(\theta) - h(x')^2 \tan(\theta) - 2x'h^2}{1 + h^2 - (x')^2 + 2x'h \tan(\theta)} \\ &= \frac{d^3 + 2h^2w + 2d^2w + dw^2 + h^2d - d}{w^2 - d^2 - h^2 - 1} \end{aligned} \quad (5)$$

Finally, we can calculate w' by using the relationship $w' = d' + x'$, which gives:

$$\begin{aligned} w' &= w + d + \frac{d^3 + 2h^2w + 2d^2w + dw^2 + h^2d - d}{w^2 - d^2 - h^2 - 1} \\ &= \frac{w^3 + d^2w + h^2w + 2dw^2 - w - 2d}{w^2 - d^2 - h^2 - 1} \end{aligned} \quad (6)$$

We will now show the existence of a second invariant denoted a^2 , as a will later be shown to be the semi-axis of an ellipse.

Proposition 3.1. *The quantity $a^2 := \frac{h^2w^2+d^2}{h^2+d^2} \in (-1, 1)$ is preserved under dynamics. That is,*

$$\frac{h^2w^2 + d^2}{h^2 + d^2} = \frac{h^2(w')^2 + (d')^2}{h^2 + (d')^2}.$$

The proof involves substituting w' and d' into the equation for a^2 to get $(a')^2 = \frac{h^2(w')^2 + (d')^2}{h^2 + (d')^2}$. After using (5) and (6) to simplify, we obtain:

$$\begin{aligned}(a')^2 &= \frac{(h^2w^2 + d^2)(p(w, h, d))}{(h^2 + d^2)(p(w, h, d))} \\ &= \frac{h^2w^2 + d^2}{h^2 + d^2} = a^2,\end{aligned}$$

where

$$\begin{aligned}p(w, h, d) &= d^4 + h^4 + 2d^2h^2 + 4d^3w + 6d^2w^2 + 4dh^2w \\ &\quad + 4dw^3 + w^4 + 2h^2w^2 - 4dw - 2w^2 + 1 + 2h^2 - 2d^2.\end{aligned}$$

□

Related to this is an equivalent invariant:

$$b^2 = \frac{h^2w^2 + d^2}{1 - w^2} = \frac{h^2a^2}{1 - a^2}.$$

3.3 Invariant Ellipses

In our altered coordinate system, the invariants a and b are actually the semi-axes of an invariant ellipse in the (w, h, d) coordinate system.

Proposition 3.2. *Let $w, h, d \in \mathbb{R}$. Recalling the definitions $a^2 = \frac{h^2w^2 + d^2}{h^2 + d^2}$ and $b^2 = \frac{h^2w^2 + d^2}{1 - w^2}$, we have $\frac{w^2}{a^2} + \frac{d^2}{b^2} = 1$ (when $a^2, b^2 \neq 0$).*

Proof.

$$\begin{aligned}\frac{w^2}{a^2} + \frac{d^2}{b^2} &= \frac{w^2}{\frac{h^2w^2 + d^2}{h^2 + d^2}} + \frac{d^2}{\frac{h^2w^2 + d^2}{1 - w^2}} \\ &= \frac{h^2w^2 + d^2w^2 + d^2 - d^2w^2}{h^2w^2 + d^2} \\ &= 1\end{aligned}$$

□

By Proposition 3.1, we have that $a^2 = (a')^2$, and by the relationship between a and b we have that $b^2 = (b')^2$. Together with Proposition 3.2, we get

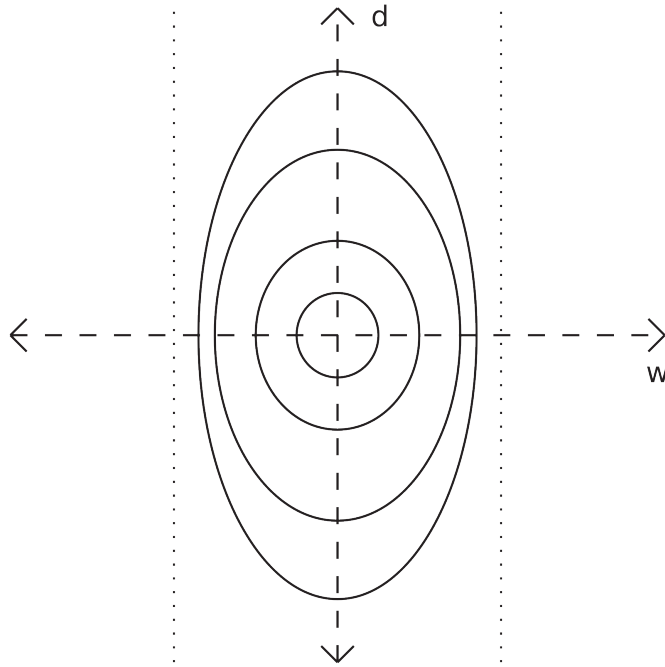


Figure 3: Several Invariant Ellipses with Height One

$$\frac{(w')^2}{a^2} + \frac{(d')^2}{b^2} = 1,$$

thus showing that any orbit belongs to an ellipse in the (w, d) -coordinate system.

Note that if a or b are equal to zero, then the other must be as well by the equation relating them. If they are both zero, we have that $w = d = 0$ for all points in the orbit. Using (3), this implies that $x = \theta = 0$ for all points in the orbit, which means such initial conditions correspond to fixed points.

3.4 Twist Dynamics

For this section, we will fix a height h and an invariant ellipse, thereby fixing invariants a and b , which are defined to be the positive square roots of a^2 and b^2 , respectively. We can parameterize the ellipse with $r(\theta) = (w, d) = (a \cos(\theta), b \sin(\theta))$. We now define the

function $\bar{f} : S^1 \rightarrow S^1$ as $\bar{f} = r^{-1} \circ f \circ r$, which allows us to view the restriction of f to our invariant ellipse as a circle diffeomorphism.

Theorem 3.3. *There exists some $\varphi \in S^1$ such that $\bar{f}(\theta) = \theta + \varphi$, where $\varphi = \varphi(a)$ is a strictly increasing function, $\varphi'(a) > 0$ given by:*

$$\varphi(a) = \begin{cases} \arctan(\frac{2ab}{b^2-a^2}) + \pi & a < b \\ \arctan(\frac{2ab}{b^2-a^2}) & a > b \\ \frac{3\pi}{2} & a = b \end{cases}$$

with

$$\varphi'(a) = \frac{2b}{b^2 + a^2}.$$

The proof of this theorem is computational and will be included in the Appendix B.

3.5 Periodic Orbits for the Billiard on the Segment

Clearly, the middle perpendicular (the y -axis) gives a 1-parameter family of fixed points (these correspond to degenerate ellipses with $a = b = 0$). Points of higher period are due to rational rotation numbers and come in 2-parameter families as one can vary the height as well.

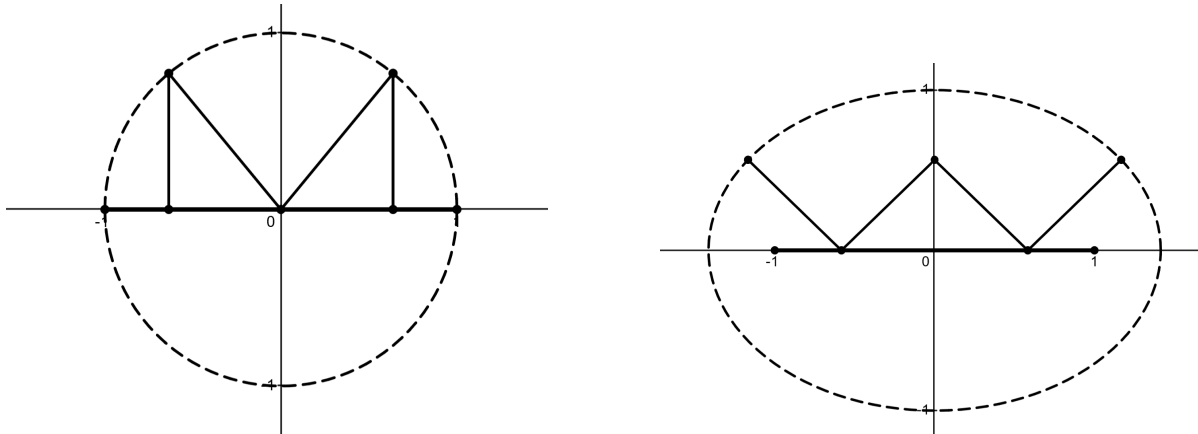


Figure 4: “M” and “W” period 4 orbits

We point out two aesthetically pleasing sub-families of period 4 orbits on Figure 4. The M -orbits fill out a semi-circle and the W -orbits fill out a semi-ellipse. For the “W” case on the right, the horizontal semi-axis is $\sqrt{2}$ and the foci of this ellipse are the ± 1 endpoints of the segment.

It is easy to calculate from the formula for the rotation number in Theorem 1.3 that for a given height h the interval of possible rotation numbers φ has the form $(\pi, \rho(h))$, where ρ is an explicit decreasing function, $\rho(h) \rightarrow 0, h \rightarrow \infty$; $\rho(h) \rightarrow 2\pi, h \rightarrow 0$. In particular, $(\pi, \rho(h)) \subset (\pi, 2\pi)$ and, hence, there are no orbits of period 2. Clearly, for all sufficiently small heights orbits of all periods ≥ 3 are present. As height increases smaller period orbits begin to disappear. For example orbits of period 4 with rotation number $\frac{3\pi}{2}$ disappear at $h = 1$ and orbits of period 3 with rotation number $\frac{4\pi}{3}$ disappear at $h \simeq 1.8$.

The explicit formula of Theorem 1.3 allows to explicitly calculate periodic orbits. For example, if one wished to find periodic orbits of least period 7, one can calculate parameter values that correspond to the rotation number $\frac{10\pi}{7}$.

Figure 5 depicts a family of period seven orbits of height one. Note that the depicted orbit is symmetric about the line $x = 0$, which unfolds into the family of asymmetric period seven orbits as indicated on the figure.

4 Numerical Simulations

4.1 Bouncing on Parabola Arcs

After fully understanding the dynamics on the segment, we can perturb the dynamics and examine how integrability is being destroyed. Probably the simplest way is to consider the unfolding of the segment into a piece of a downward-facing parabola given by $f(x) = -ax^2 + a$ $\{-1 \leq x \leq 1\}$. We will make a slight modification to our visibility domain to make sure that bouncing billiard still makes sense.

Recall that our definition required that for (p, v) in the visibility domain, the ray

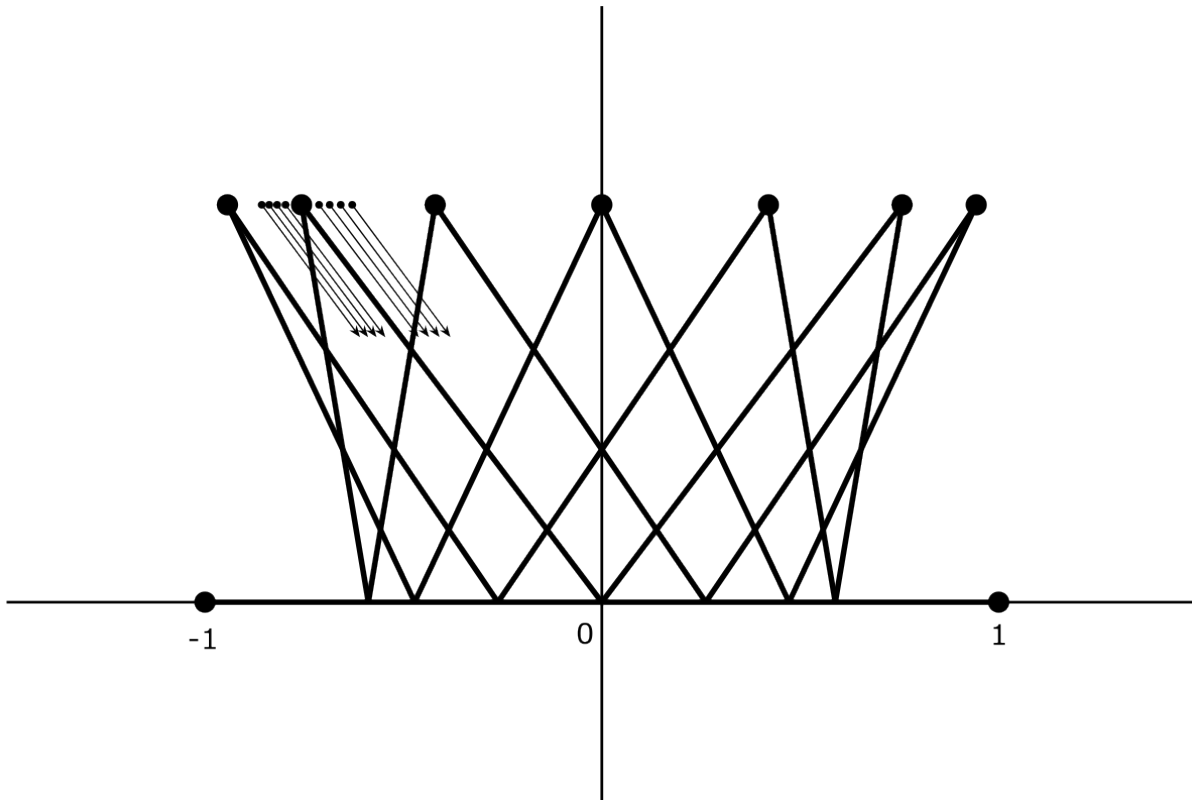


Figure 5: Family of Orbits of Period 7

spanned by v has a nonempty intersection with the boundary of the set. For the parabola, we will require that the ray has a nonempty intersection with the parabola, but we will impose the additional requirement that the segment \overline{pw} lies entirely above the parabola given by $-ax^2 + a$, where w is the closest intersection point to p of the ray and parabola. In other words, a point p must not be able to “see” the underside of the parabola. The dynamics rule remains the same, simply utilizing the newly defined visibility domain for the visibility angle reflection.

Remark 4.1. *Despite the fact that our integrable model is a perfect twist map, KAM theory doesn’t apply directly since we are in a 3-dimensional situation. Still, as we see below, KAM features such as elliptic islands seem to be present in our unfolding.*

Figure 6 depicts some orbits on a parabola of height $\frac{3}{10}$. We observe that most of the orbits that begin close to the parabola fill invariant arcs which align themselves along the parabola (see the red orbit marked with a (2) in the figure). Others, such as the blue (1) and yellow (3) orbits, fill up periodic curves. Finally, some orbits, such as the black (4) one, exhibit more complicated behavior similar to Aubry-Mather sets with positive Lyapunov exponent.

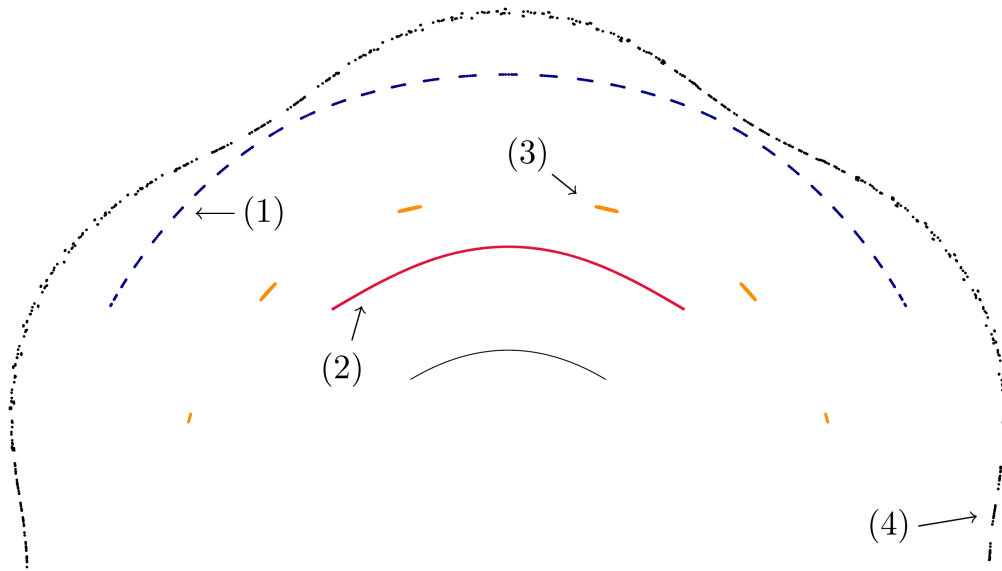


Figure 6: Orbits on Parabola of Height $\frac{3}{10}$

As we increase the height, the observed behaviors become more complicated. Figure 7 and Figure 8 depict orbits on parabolas of heights $\frac{1}{2}$ and 1, respectively. On these more extreme parabolas, we still observe periodic curves which take more complicated shapes, including non-symmetric orbits such as the blue (1) orbit on Figure 8. Additionally, with increased height, we more easily detect chaotic behavior, such as the black (4) orbits of both figures and the yellow (3) orbit of Figure 8.

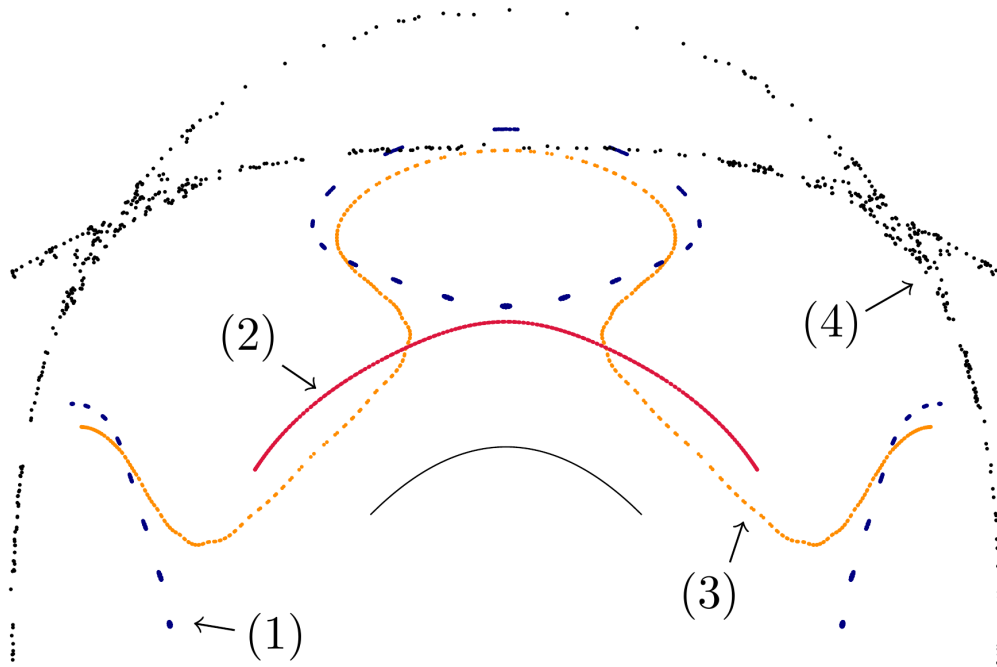


Figure 7: Orbits on Parabola of Height $\frac{1}{2}$

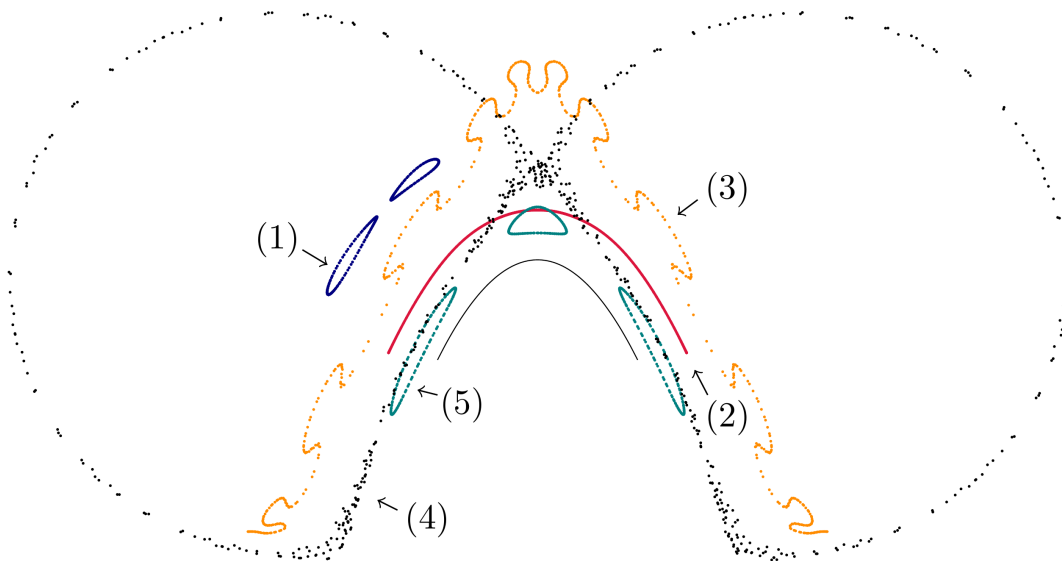


Figure 8: Orbits on Parabola of Height 1

4.2 Bouncing on the Square

It is also interesting to investigate bouncing billiards on polygons. For the sake of simplicity, we will focus solely on the system on the square. On the square, we classify observed orbits into five categories.

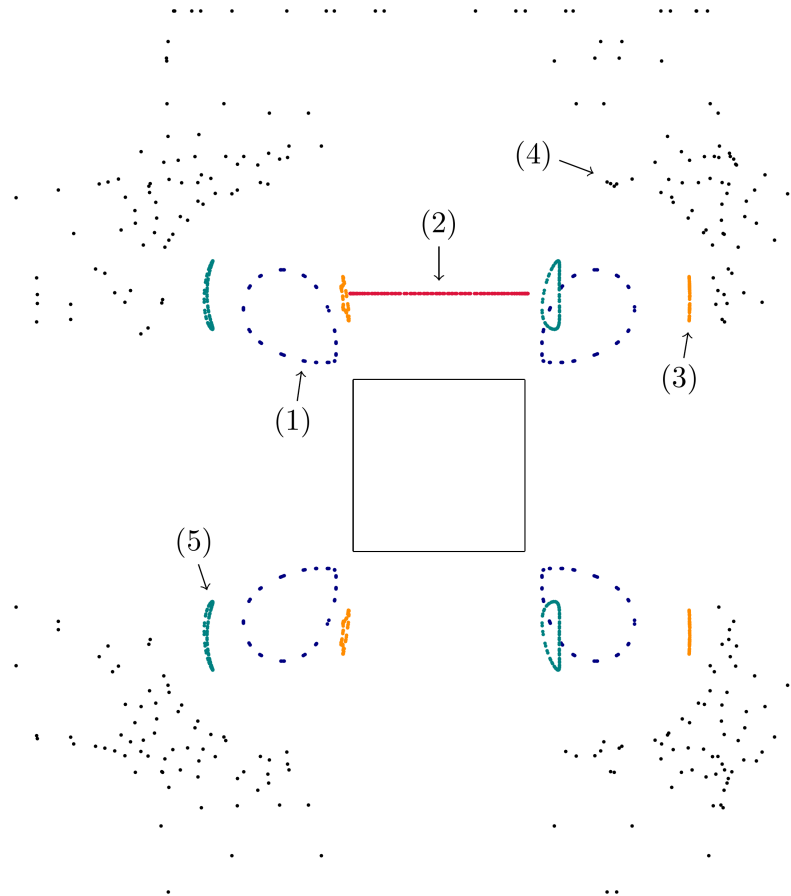


Figure 9: Orbits on a Square

The first category, such as the red (2) orbit in Figure 9, consists of points staying a fixed perpendicular distance away from one side of the square. For some such orbits, the orbit never extend in the direction parallel to that side further than the endpoints of the side. In this case, the system is identical to that on the line segment. In other cases, such orbit can extend past the corners of the square while still remaining on one side; in this

case the orbit is not the same as an orbit on the segment.

The second kind are those orbits which fill up four closed curves, with one near each corner of the square. This can be seen in the cyan (5) orbit of Figure 9. Most of these orbits observed appeared to be rotationally symmetric, but the one pictured is not.

The third kind involves what appears to be an invariant loop near each corner, but actually consists of many smaller closed curves making up the apparent larger circle. This is depicted in the blue (1) orbit of the figure.

The fourth kind is another chaotic variety. It involves a period 4 non-smooth set, possibly a Cantor set. This kind is depicted in the yellow (3) orbit of the figure.

The final class of orbits occupy all sides of the square and seem to behave chaotically such as the black (4) orbit. Such orbits appear to fill up positive area domains. However, numerics become very tricky for such orbits, as we clearly detected positive Lyapunov exponents for such orbits.

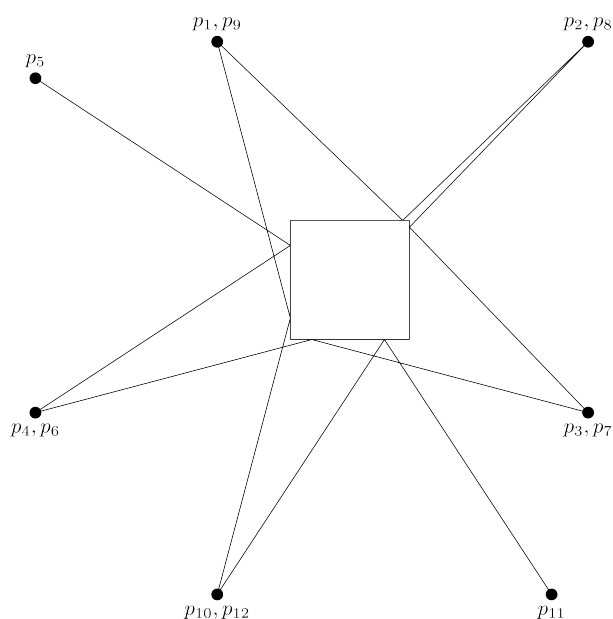


Figure 10: Period Twelve Orbit on Square with Large Eigenvalue

Another finding on the square is the existence of periodic points whose Jacobian

matrix has eigenvalues greater than one. Figure 10 shows one such example. It depicts a period twelve orbit whose Jacobian matrix has eigenvalues approximately 0.086, 1, and 11.592.

Remark 4.2. *It is easy to see from the form of the differential of the bouncing outer billiard on a convex polygon that every periodic point of such a billiard has at least one eigenvalue equal to 1.*

4.3 Bouncing on an Ellipse

While we fully understand the segment and the circle, in between fall ellipses, which also show very complex behavior. We consider bouncing outer billiard on the ellipse with major and minor semi-axis equal to 1 and 0.4, respectively. As expected, we can have orbits which are similar to the segment and circle, as shown in Figure 11 and Figure 12, respectively.

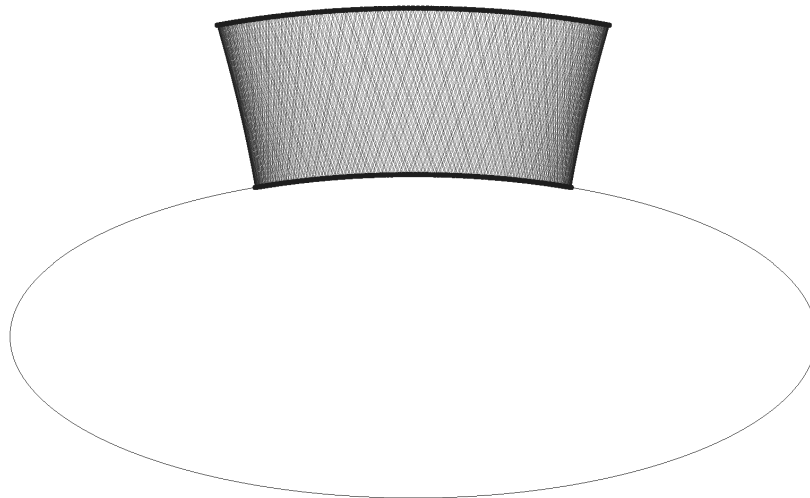


Figure 11: Segment-like behavior

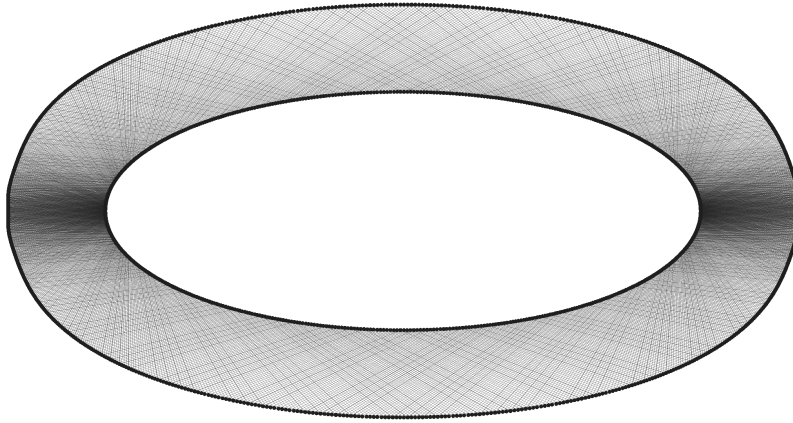


Figure 12: Circle-like behavior

We also have cases where the orbit closure fill periodic closed curves, such as those in Figure 13 and Figure 14.

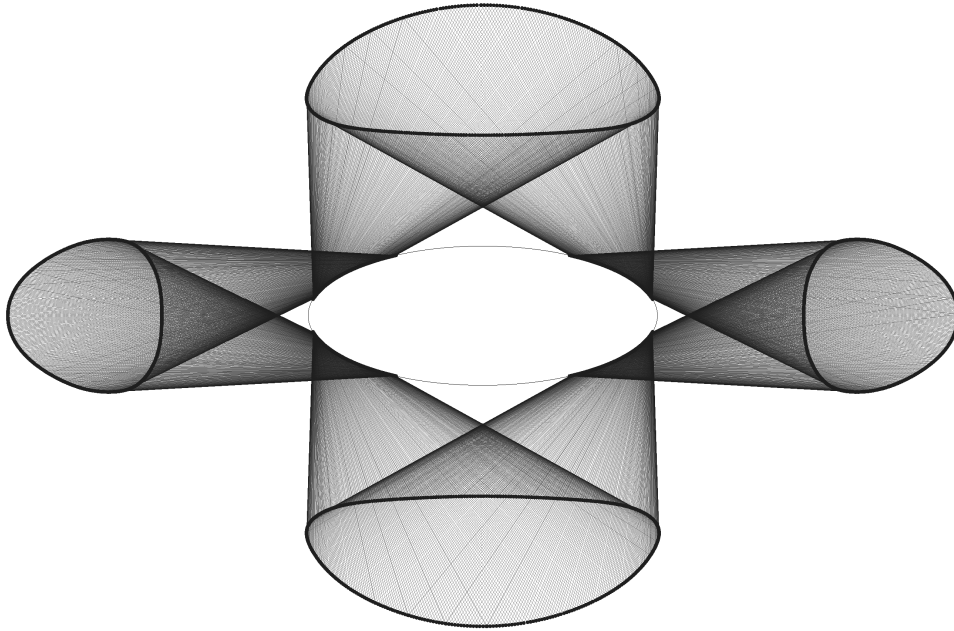


Figure 13: Four closed invariant curves

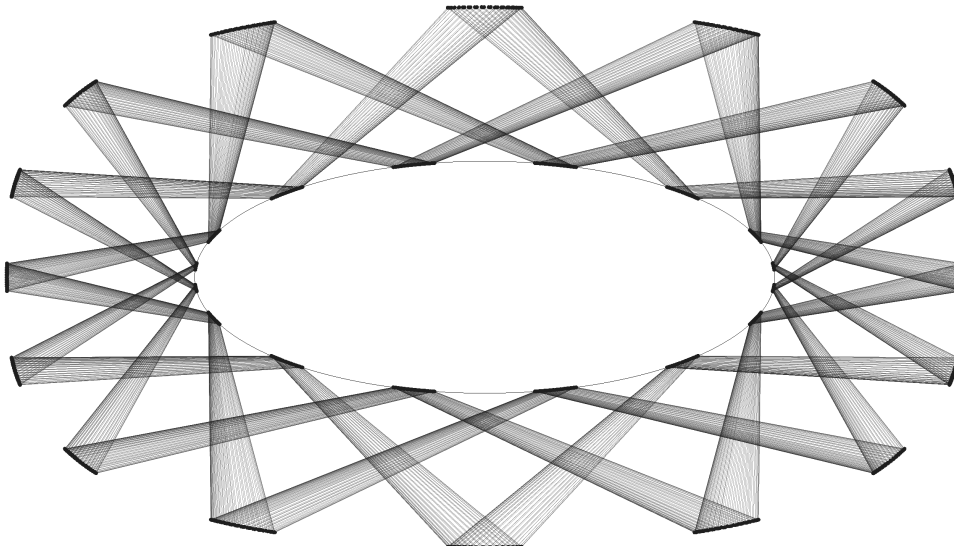


Figure 14: Many closed invariant curves

Finally, “in between” the circle-like behavior and four closed curve behavior, we detect an orbit which appears to fill up positive area domain, as shown in Figure 15.

We notice that the types of orbits we observe for the parabola arc and the ellipse are the same.

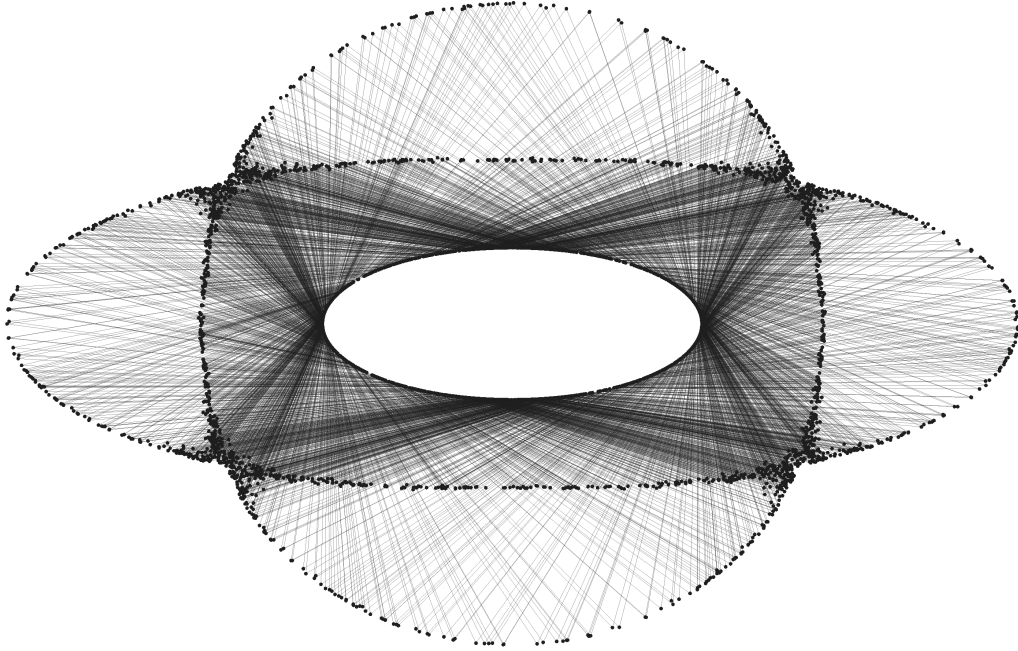


Figure 15: A chaotic orbit

Appendix A: The Conservative Property

Here we verify that bouncing outer billiard dynamics F preserves the Lebesgue measure. Let dA be the standard 2-dimensional Lebesgue measure restricted to \mathbb{R}^2 and let $d\theta$ be the Lebesgue on the circle.

Proposition 4.3. *Assume that the boundary of S is a C^2 curve; then the restriction of $dA \otimes d\theta$ to V_S is an infinite measure which is invariant under F .*

Remark 4.4. *It is easy to verify invariance of the Lebesgue measure for polygons and seems*

likely to be true for any convex S , but we haven't verified it in such generality.

Proof. We begin by noticing that the proposition holds true if S is a closed disc. Indeed, in this case it is easy to see that the visibility domain can be decomposed into circles on each of which F is a rigid rotation preserving the length (conditional measure). Hence F preserves $dA \otimes d\theta$.

Now, given a general domain S with C^2 boundary, we will verify that F_S is measure-preserving by checking that the Jacobian $JF = \det(DF)$ equals 1. Let $(p, v) \in V_S$, we can assume that (p, v) is in fact in the interior of V_S since ∂V_S has measure zero. Therefore, the ray starting at v intersect ∂S at the bounce point w transversely. This implies that infinitesimal variations of (p, v) result in infinitesimal variations of w of the same order of magnitude.

Consider the (unique) closed disc D such that ∂D is tangent to ∂S at w to the second order. Clearly, we have $F_S(p, v) = F_D(p, v)$. In fact, second-order tangency ensures that $DF_S(p, v) = DF_D(p, v)$. Indeed, to see this, first note that infinitesimal variation of (p, v) results in infinitesimal variations of w (on ∂S and ∂D), agreeing up to the second order. The angles of reflection of w are controlled by the derivatives of ∂S and ∂D at w and, hence, agree up to the first order (again due to second-order tangency at w) and the claim follows. Hence we have

$$JF_S(p, v) = \det DF_S(p, v) = \det DF_D(p, v) = 1,$$

where the last equality is by measure-preserving property of F_D pointed out at the beginning of the proof.

It is easy to show that the total Lebesgue measure of V_S is infinite when integrating in the correct order. For any angle θ , there is an infinitely long strip of constant width w of points whose rays at angle θ will hit S , where w is the length of S projected onto the axis perpendicular to θ . \square

Alternatively, one can verify the above proposition by a direct calculation of $DF(p, v)$ without any reference to the disc case. Specifically, we can center the (x, y) -coordinate

system at the bounce point w so that the x -axis is tangent to ∂S and denote by θ the circular coordinate. We write $(p, v) = (a, b, \theta_0)$. Clearly $dA \otimes d\theta = dx \otimes dy \otimes d\theta$ and we need to verify that the Jacobian is 1 in (x, y, θ) -coordinates. Prior to the last visibility angle reflection step we have $(a, b, \theta_0) \mapsto (-a, b, -\theta_0)$ and a routine calculation gives the following expression for its derivative:

$$\begin{pmatrix} 1 + 2kb & -2ka - \frac{2a}{b} & \frac{2c^2}{b} + 2kc^2 \\ 2ka & 1 - \frac{2ka^2}{b} & \frac{2kac^2}{b} \\ -2k & \frac{2ka}{b} & -1 - \frac{2kc^2}{b} \end{pmatrix}$$

where k is the curvature at w and $c = \sqrt{a^2 + b^2}$. The determinant of this matrix is -1 , which becomes 1, after composing with the reflection $\theta \mapsto \text{const} - \theta$ according to the visibility angle reflection rule.

Appendix B: Proof of Theorem 3.3

First, we will find an explicit formula for $r^{-1}(w, d)$ for w and d lying on the ellipse. We have $w = a \cos(\theta)$ and $d = b \sin(\theta)$, meaning $\tan(\theta) = \frac{ad}{bw}$. This yields:

$$\theta = r^{-1}(w, d) = \arctan\left(\frac{ad}{bw}\right) + \pi n(w) \quad (7)$$

In this formula, we use

$$n(x) := \begin{cases} 1 & x < 0 \\ 0 & x \geq 0 \end{cases}$$

to compensate for the fact that \arctan only outputs between $-\frac{\pi}{2}$ to $\frac{\pi}{2}$. This explicit formula has the slight flaw that it fails for $w = 0$. However, it can be shown separately that this case matches the behavior of all other cases. Applying r^{-1} to the right of both sides of the equation $\bar{f} = r^{-1} \circ f$ or yields $\bar{f} \circ r^{-1}(w, d) = r^{-1} \circ f(w, d) = r^{-1}(w', d')$. Applying (7) yields:

$$\bar{f}\left(\arctan\left(\frac{ad}{bw}\right) + \pi n(w)\right) = \arctan\left(\frac{ad'}{bw'}\right) + \pi n(w')$$

Thus $\overline{f}(\theta) = \theta + \varphi(w, d)$, where

$$\varphi(w, d) = \arctan\left(\frac{ad'}{bw'}\right) + \pi n(w') - \arctan\left(\frac{ad}{bw}\right) - \pi n(w).$$

We will first show that $\varphi(w, d)$ is constant mod π . The terms $\pi n(w')$ and $-\pi n(w)$ are equivalent to zero mod π , so we will revisit these later.

Thus, we currently seek to show that $\arctan(\frac{ad'}{bw'}) - \arctan(\frac{ad}{bw})$ is constant mod π . We will use the arc-tangent subtraction formula $\arctan(x) - \arctan(y) = \arctan(\frac{x-y}{1+xy}) + m\pi$, where m is either 0 or 1 depending on x and y . The term $m\pi$ is equivalent to zero mod π in all cases, so we will revisit this term later as well.

For the purposes of the following calculation, we will set $x = \frac{ad'}{bw'}$ and $y = \frac{ad}{bw}$. Our goal is to show that $\frac{x-y}{1+xy}$ is constant for any w and d on the fixed ellipse. First, since x and y each have a factor of $\frac{a}{b}$, which is constant for points on the ellipse, we can pull this out of the fraction:

$$\frac{x-y}{1+xy} = \left(\frac{a}{b}\right) \left(\frac{\frac{d'}{w'} - \frac{d}{w}}{1 + \frac{a^2 dd'}{b^2 ww'}} \right)$$

Next, multiply the numerator and denominator by $b^2 ww'$ to get:

$$\left(\frac{a}{b}\right) \left(\frac{b^2 d' w - b^2 d w'}{b^2 ww' + a^2 dd'} \right)$$

We can pull out another b^2 to bring the total constant factored out to ab :

$$(ab) \left(\frac{d' w - d w'}{b^2 ww' + a^2 dd'} \right)$$

After replacing w' and d' with their equivalent expressions in terms of w , h , and d , then multiplying the numerator and denominator by $(w^2 - d^2 - h^2 - 1)$, we get:

$$\frac{(ab)(2h^2 w^2 + 2d^2)}{b^2(w^4 + d^2 w^2 + h^2 w^2 + 2dw^3 - w^2 - 2dw) + a^2(d^4 + 2dh^2 w + 2d^3 w + d^2 w^2 + d^2 h^2 - d^2)}$$

After substituting in the expressions for a^2 and b^2 , multiplying the numerator and denominator by $(1 - w^2)(h^2 + d^2)$, and simplifying, we get:

$$\frac{2ab(1 - w^2)(h^2 + d^2)}{d^2h^2w^2 + h^4w^2 + h^2w^4 + d^4 + d^2h^2 + d^2w^2 - h^2w^2 - d^2}$$

Factoring the denominator yields:

$$\frac{2ab(1 - w^2)(h^2 + d^2)}{(h^2w^2 + d^2)(h^2 + d^2) - (h^2w^2 + d^2)(1 - w^2)}$$

Finally, dividing the numerator and denominator by $(1 - w^2)(h^2 + d^2)$ gives:

$$\frac{2ab}{\frac{h^2w^2+d^2}{1-w^2} - \frac{h^2w^2+d^2}{(h^2+d^2)}} = \frac{2ab}{b^2 - a^2}$$

Thus, we end up with the equation:

$$\varphi = \arctan\left(\frac{2ab}{b^2 - a^2}\right) \bmod \pi$$

Next, we will go back and carefully consider each of the extra terms we set aside earlier to show that φ is actually constant mod 2π . Each of these components individually may depend on w, d, a , and b , but we will show that together they only depend on a and b , which remain constant within an orbit.

We will begin with the term denoted as $m\pi$ earlier. Recall that this arose out of the extra term from the arc-tangent sum formula. Again using the definitions $x = \frac{ad'}{bw'}$ and $y = \frac{ad}{bw}$, we get that $m = 0$ if $-xy < 1$ and $m = 1$ if $-xy > 1$. This is equivalent to saying $m = 0$ if $1 + xy > 0$ and $m = 1$ if $1 + xy < 0$. After substituting in expressions to get $1 + xy$ in terms of w, h , and d as well as simplifying and factoring, we get:

$$1 + xy = \frac{(d^2 + h^2w^2)(d^2 + h^2 + w^2 - 1)}{(d^2 + h^2)(d^2w^2 + h^2w^2 + 2dw^3 + w^4 - 2dw - w^2)}$$

Since we are only concerned about the sign of $1 + xy$, and $\frac{d^2+h^2w^2}{d^2+h^2} \geq 0$, we can factor this out and ignore it. This leaves us with:

Bouncing Outer Billiards

$$\frac{d^2 + h^2 + w^2 - 1}{d^2w^2 + h^2w^2 + 2dw^3 + w^4 - 2dw - w^2} = \frac{d^2 + h^2 + w^2 - 1}{w^2(d^2 + h^2 + w^2 - 1) + 2dw^3 - 2dw}$$

This has the same sign as its reciprocal, which after simplification becomes:

$$w^2 + \frac{2dw^3 - 2dw}{d^2 + h^2 + w^2 - 1}$$

Next, it will benefit us to rewrite d in terms of w , a , and b . Starting from the ellipse equation $\frac{w^2}{a^2} + \frac{d^2}{b^2} = 1$, we can derive the equation $d^2 = b^2 - \frac{w^2b^2}{a^2}$. Rewriting our previous expression yields:

$$w^2 + \frac{(2w^3 - w) \left(\pm \sqrt{b^2 - \frac{w^2b^2}{a^2}} \right)}{b^2 - \frac{w^2b^2}{a^2} + h^2 + w^2 - 1}$$

Next, we will remove h from the expression. Recall the relationship between a^2 and b^2 given by $b^2 = \frac{h^2a^2}{1-a^2}$. From this, we can derive $h^2 = \frac{b^2-a^2b^2}{a^2}$. From here, we can perform a series of simplifications:

$$\begin{aligned} w^2 + \frac{(2w^3 - w) \left(\pm \sqrt{b^2 - \frac{w^2b^2}{a^2}} \right)}{b^2 - \frac{w^2b^2}{a^2} + h^2 + w^2 - 1} &= w^2 + \frac{2w(w^2 - 1) \left(\pm \sqrt{b^2 - \frac{w^2b^2}{a^2}} \right)}{\frac{b^2}{a^2} - \frac{w^2b^2}{a^2} + \frac{w^2a^2}{a^2} - \frac{a^2}{a^2}} \\ &= w^2 + \frac{2wa^2(w^2 - 1) \left(\pm \sqrt{\frac{b^2(a^2 - w^2)}{a^2}} \right)}{(w^2 - 1)(a^2 - b^2)} \\ &= w^2 + \frac{2wab(\pm \sqrt{a^2 - w^2})}{a^2 - b^2} \\ &= \frac{a^2w^2 - b^2w^2 + 2wab(\pm \sqrt{a^2 - w^2})}{a^2 - b^2} \end{aligned}$$

Next, we want to find the zeros of this expression with respect to w . Clearly, $w = 0$ is a zero. To find other zeros, we will set the numerator of our expression equal to zero and assume $w \neq 0$. $a^2w^2 - b^2w^2 + 2wab(\pm \sqrt{a^2 - w^2}) = 0 \Rightarrow a^2w - b^2w + 2ab(\pm \sqrt{a^2 - w^2}) = 0$. After rearranging and squaring both sides, we get:

$$a^2 - w^2 = \frac{b^4w^2 - 2a^2b^2w^2 + a^4w^2}{4a^2b^2}$$

Solving for w yields:

$$w = \pm \frac{2a^2b}{a^2 + b^2}$$

From this point forward, we will assume d is positive. The calculations play out similarly if d is negative, and the results will be given with the positive case. This means our fraction is zero when $a^2w - b^2w + 2ab\sqrt{a^2 - w^2} = 0$, removing the plus or minus present earlier. We have the possible zeros of $\pm \frac{2a^2b}{a^2+b^2}$, but determining which is a true zero will depend on the values of a and b . This is because $\sqrt{a^2 - w^2}$ becomes $\frac{a(a^2-b^2)}{a^2+b^2}$ if $a > b$ or $\frac{a(b^2-a^2)}{a^2+b^2}$ if $a < b$. This means that if $a > b$ we have $\frac{-2a^2b}{a^2+b^2}$ is a zero, whereas if $b > a$ we have $\frac{2a^2b}{a^2+b^2}$ is a zero.

To find the sign of the expression, we can solve the derivatives at the zeros:

$$\frac{d}{dw} \left(\frac{a^2w^2 - b^2w^2 + 2wab\sqrt{a^2 - w^2}}{a^2 - b^2} \right) = \frac{2a^2w - 2b^2w + 2ab\sqrt{a^2 - w^2} - \frac{2abw^2}{a^2 - w^2}}{a^2 - b^2} \quad (8)$$

We will first analyze the derivative values for $a > b$. The denominator is positive in this case, and we see that the derivative is positive at $w = 0$. For $w = \frac{-2a^2b}{a^2+b^2}$, we have that the numerator of (8) becomes:

$$\frac{2a^2b(b^2 - a^2)}{a^2 + b^2} + \frac{-2abw^2}{a^2 - w}$$

The second term of this expression is always negative. Since we assumed $a > b$, the first term is also negative, meaning the derivative is negative for this w -value.

In the case where $a < b$, the denominator is always negative, and we have that the derivative is negative at $w = 0$. For $w = \frac{2a^2b}{a^2+b^2}$, the numerator becomes:

$$\frac{2a^2b(a^2 - b^2)}{a^2 + b^2} + \frac{-2abw^2}{a^2 - w}$$

This is again negative, but the derivative is positive, since the denominator of (8) is negative. In summary, we have the following results:

In $d > 0$ Case: If $a < b$ and $w \in (\frac{2a^2b}{a^2+b^2}, 1] \cup [-1, 0)$, then $1 + xy > 0$.
 If $a < b$ and $w \in (0, \frac{2a^2b}{a^2+b^2})$, then $1 + xy < 0$.
 If $a > b$ and $w \in [-1, \frac{-2a^2b}{a^2+b^2}) \cup (0, 1]$, then $1 + xy > 0$.
 If $a > b$ and $w \in (\frac{-2a^2b}{a^2+b^2}, 0)$, then $1 + xy < 0$.

The case where $d < 0$ works similarly, with results as follows:

In $d < 0$ Case: If $a < b$ and $w \in [-1, \frac{-2a^2b}{a^2+b^2}) \cup (0, 1]$, then $1 + xy > 0$.
 If $a < b$ and $w \in (\frac{-2a^2b}{a^2+b^2}, 0)$, then $1 + xy < 0$.
 If $a > b$ and $w \in (\frac{2a^2b}{a^2+b^2}, 1] \cup [-1, 0)$, then $1 + xy > 0$.
 If $a > b$ and $w \in (0, \frac{2a^2b}{a^2+b^2})$, then $1 + xy < 0$.

Next, we will tackle the $\pi n(w')$ term. Recall that $n(w')$ is defined to be 1 when w' is negative and 0 otherwise. Thus, our next goal is to determine the sign of w' under all possible conditions. We will again take $d > 0$ and present the results for the $d < 0$ case later.

$$\begin{aligned}
 w' &= \frac{w^3 + d^2w + h^2w + 2dw^2 - w - 2d}{w^2 - d^2 - h^2 - 1} \\
 &= \frac{w^3 - \frac{b^2w^3}{a^2} + \frac{b^2w}{a^2} + 2w^2\sqrt{b^2 - \frac{b^2w^2}{a^2}} - w - 2\sqrt{b^2 - \frac{b^2w^2}{a^2}}}{w^2 + \frac{b^2w^2}{a^2} - \frac{b^2}{a^2} - 1} \\
 &= \frac{(w^2 - 1)(a^2w - b^2w + 2ab\sqrt{a^2 - w^2})}{(w^2 - 1)(a^2 + b^2)} \\
 &= \frac{a^2w - b^2w + 2ab\sqrt{a^2 - w^2}}{a^2 + b^2}
 \end{aligned} \tag{9}$$

We have already examined the zeros of this expression when working through the $m\pi$ term. It has a zero at $w = \frac{2a^2b}{a^2+b^2}$ when $a < b$ and one at $\frac{-2a^2b}{a^2+b^2}$ when $a > b$. Notably, this expression does not have a zero at $w = 0$ like the previous. In this case, we have that the

derivative is negative at $w = \frac{2a^2b}{a^2+b^2}$ when $a < b$ and positive at $\frac{-2a^2b}{a^2+b^2}$ when $a > b$.

In $d > 0$ Case: If $a < b$ and $w \in [-1, \frac{2a^2b}{a^2+b^2})$, then $w' > 0$.

If $a < b$ and $w \in (\frac{2a^2b}{a^2+b^2}, 1]$, then $w' < 0$.

If $a > b$ and $w \in (\frac{-2a^2b}{a^2+b^2}, 1]$, then $w' > 0$.

If $a > b$ and $w \in [-1, \frac{-2a^2b}{a^2+b^2})$, then $w' < 0$.

Similarly, if $d < 0$, we get:

In $d < 0$ Case: If $a < b$ and $w \in [-1, \frac{-2a^2b}{a^2+b^2})$, then $w' > 0$.

If $a < b$ and $w \in (\frac{-2a^2b}{a^2+b^2}, 1]$, then $w' < 0$.

If $a > b$ and $w \in (\frac{2a^2b}{a^2+b^2}, 1]$, then $w' > 0$.

If $a > b$ and $w \in [-1, \frac{2a^2b}{a^2+b^2})$, then $w' < 0$.

Finally, we have the $-\pi n(w)$ term, which requires no extra analysis since our results are currently allowed to be dependent on w .

The final step in this proof is to check how many π terms are added for each initial condition for w and d , as well as a and b values. This will be omitted since it solely involves going through each relevant interval for w and d for both the $a > b$ and $a < b$ case. The results are as follows:

$$\varphi = \begin{cases} \arctan(\frac{2ab}{b^2-a^2}) + \pi & a < b \\ \arctan(\frac{2ab}{b^2-a^2}) & a > b \\ \frac{-\pi}{2} & a = b \end{cases}$$

Taking the derivative of φ with respect to a yields:

$$\varphi'(a) = \frac{2b}{b^2 + a^2}$$

This is clearly positive for all values $a > 0$ since b is nonzero and positive for such a . \square

References

- [Mos73] J. Moser. *Stable and Random Motions in Dynamical Systems*, volume 77 of *Annals of Mathematics Studies*. Princeton University Press, 1973. 117
- [Mos78] J. Moser. Is the solar system stable? *Mathematical Intelligencer*, 1:65–71, 1978. 117
- [Neu58] B. H. Neumann. Sharing ham and eggs. *Iota.*, pages 14–18, 1958. 117
- [Tab95] S. Tabachnikov. On the dual billiard problem. *Adv. Math.*, 115(2):221–249, 1995. 119
- [Tab12] S. Tabachnikov. The (un)equal tangents problem. *The American Mathematical Monthly*, 119(5):398–405, 2012. 123

AUTHORS

Andrey Gogolev
Department of Mathematics,
The Ohio State University,
Columbus, OH, USA, 43210
email: gogolyev.1@osu.edu

Levi Keck
Department of Mathematics,
The Ohio State University,
Columbus, OH, USA, 43210
email: keck.140@osu.edu

Andrey Gogolev, Levi Keck, Kevin Lewis

Kevin Lewis

Department of Mathematics,

The Ohio State University,

Columbus, OH, USA, 43210

email: lewis.3164@osu.edu